



A Novel Low-Cost, High-Resolution Camera System for Measuring Peat Subsidence and Water Table Dynamics

Chris D. Evans^{1*}, Nathan Callaghan¹, Adi Jaya², Alistair Grinham³, Sofie Sjogersten⁴, Susan E. Page⁵, Mark E. Harrison^{5,6}, Kitso Kusin⁷, Lip Khoon Kho⁸, Martha Ledger⁴, Stephanie Evers^{9,10}, Zak Mitchell¹, Jennifer Williamson¹, Alan D. Radbourne¹ and A. Jonay Jovani-Sancho^{1,4}

¹United Kingdom Centre for Ecology and Hydrology, Bangor, United Kingdom, ²Faculty of Agriculture, University of Palangka Raya, Palangkaraya, Indonesia, ³School of Civil Engineering, The University of Queensland, Brisbane, QLD, Australia, ⁴School of Biosciences, University of Nottingham, Loughborough, United Kingdom, ⁵School of Geography, Geology and the Environment, University of Leicester, Leicester, United Kingdom, ⁶Centre for Ecology and Conservation, College of Life and Environmental Sciences, University of Exeter, Penryn, United Kingdom, ⁷Center for International Cooperation in Sustainable Management of Tropical Peatland (CIMTROP), University of Palangka Raya, Palangkaraya, Indonesia, ⁸Peat Ecosystem and Biodiversity Unit, Biology and Sustainability Research Division, Malaysian Palm Oil Board, Kuala Lumpur, Malaysia, ⁹School of Biological and Environmental Sciences, Liverpool John Moores University, Liverpool, United Kingdom, ¹⁰School of Environmental and Geographical Sciences, University of Nottingham Malaysia Campus, Selangor, Malaysia

OPEN ACCESS

Edited by:

Massimo Lupascu,
National University of Singapore,
Singapore

Reviewed by:

Baptiste Dafflon,
Lawrence Berkeley National
Laboratory, United States
Sudipta Rakshit,
Tennessee State University,
United States

*Correspondence:

Chris D. Evans
cev@ceh.ac.uk

Specialty section:

This article was submitted to
Soil Processes,
a section of the journal
Frontiers in Environmental Science

Received: 24 November 2020

Accepted: 26 January 2021

Published: 22 March 2021

Citation:

Evans CD, Callaghan N, Jaya A, Grinham A, Sjogersten S, Page SE, Harrison ME, Kusin K, Kho LK, Ledger M, Evers S, Mitchell Z, Williamson J, Radbourne AD and Jovani-Sancho AJ (2021) A Novel Low-Cost, High-Resolution Camera System for Measuring Peat Subsidence and Water Table Dynamics. *Front. Environ. Sci.* 9:630752. doi: 10.3389/fenvs.2021.630752

Peatlands are highly dynamic systems, able to accumulate carbon over millennia under natural conditions, but susceptible to rapid subsidence and carbon loss when drained. Short-term, seasonal and long-term peat surface elevation changes are closely linked to key peatland attributes such as water table depth (WTD) and carbon balance, and may be measured remotely using satellite radar and LiDAR methods. However, field measurements of peat elevation change are spatially and temporally sparse, reliant on low-resolution manual subsidence pole measurements, or expensive sensor systems. Here we describe a novel, simple and low-cost image-based method for measuring peat surface motion and WTD using commercially available time-lapse cameras and image processing methods. Based on almost two years' deployment of peat cameras across contrasting forested, burned, agricultural and oil palm plantation sites in Central Kalimantan, Indonesia, we show that the method can capture extremely high resolution (sub-mm) and high-frequency (sub-daily) changes in peat surface elevation over extended periods and under challenging environmental conditions. WTD measurements were of similar quality to commercially available pressure transducers. Results reveal dynamic peat elevation response to individual rain events, consistent with variations in WTD. Over the course of the relatively severe 2019 dry season, cameras in deep-drained peatlands recorded maximum peat shrinkage of over 8 cm, followed by partial rebound, leading to net annual subsidence of up to 5 cm. Sites with higher water tables, and where borehole irrigation was used to maintain soil moisture, had lower subsidence, suggesting potential to reduce subsidence through altered land-management. Given the established link between subsidence and CO₂ emissions, these results have direct implications for the management of peatlands to reduce high

current greenhouse gas (GHG) emissions. Camera-based sensors provide a simple, low-cost alternative to commercial elevation, WTD and GHG flux monitoring systems, suitable for deployment at scale, and in areas where existing approaches are impractical or unaffordable. If ground-based observations of peat motion can be linked to measured GHG fluxes and with satellite-based monitoring tools, this approach offers the potential for a large-scale peatland monitoring tool, suitable for identifying areas of active carbon loss, targeting climate change mitigation interventions, and evaluating intervention outcomes.

Keywords: peatlands, subsidence, water table, carbon, indonesia, oil palm, smallholder farming, peat swamp forest

INTRODUCTION

Peatlands are the most carbon rich terrestrial ecosystems on earth, storing an estimated total of 637 Gt C (Page et al., 2011; Dargie et al., 2017), which is equivalent to three quarters of all the CO₂ currently in the atmosphere (860 Gt C; Friedlingstein et al., 2019). This carbon store is under unprecedented and intensifying pressure from human activities, including land conversion and drainage for agriculture and plantation forestry, grazing, and the use of fire for land clearance or management (Turetsky et al., 2015; Page and Baird, 2016). The oxidation and combustion of peat exposed to oxygen is estimated to generate around 1–2 Gt of CO₂ emissions per year (Smith et al., 2014; Leifeld and Menichetti, 2018), as well as N₂O emissions of 0.36 Gt CO₂-equivalent yr⁻¹ (FAOSTAT, 2018, based on a 100 years global warming potential of 298; Smith et al., 2014). Although partly offset by reduced CH₄ emissions as a result of wetland drainage, overall greenhouse gas (GHG) emissions resulting from human utilization of peatlands are estimated to generate in the region of 2–5% of global GHG emissions (Smith et al., 2014). Historically, the most extensive conversion and drainage of peatlands occurred in Northern Europe, with some areas having undergone large-scale change centuries ago. More recently, the tropical peatlands of Southeast Asia have undergone very rapid conversion, with 60% of the original area of peat swamp forest cleared between 1990 and 2010, the majority of which is now under drainage-based cultivation (Wijedasa et al., 2018).

An additional, and closely associated, consequence of peatland drainage is land subsidence. This occurs due to a combination of consolidation and compaction (loss of buoyancy and shrinkage resulting from removal of water from the pore space, often augmented by the use of heavy machinery during agricultural and forestry activities), together with accelerated erobic decomposition of the peat following exposure to oxygen. Initial subsidence of peat due to compaction following drainage may be very rapid (potentially >1 m within 5 years; Hooijer et al., 2012), while subsidence due to ongoing compaction and oxidation can continue for decades to centuries (e.g., Hutchinson, 1980; Stephens et al., 1984). Rates of subsidence depend on drainage depth, time since drainage and climate, with rates of subsidence in high-latitude peatlands subject to long-term drainage typically in the range 1–3 cm yr⁻¹, and those in more recently drained tropical peatlands typically 3–6 cm yr⁻¹ (Evans et al., 2019 and references therein). Apart from contributing to CO₂ emissions, the socio-economic

consequences of peat subsidence include the need to transition from low-cost gravity drainage to high-cost, energy-intensive pumped drainage; damage to buildings and linear infrastructure such as roads and pipelines; growing flood risk; and loss of agricultural productivity. Many low-lying peat areas subject to long-term drainage are now below sea-level, including parts of the The Netherlands, Eastern England and Northern Germany. In the The Netherlands alone, drainage and subsidence of peatlands has contributed to approximately 2 m of subsidence in coastal areas, most of which are now below sea-level; to an overall loss of 20 km³ of peat volume; and to CO₂ emissions sufficient to raise atmospheric CO₂ concentrations by 0.39 ppmv (Erkens et al., 2016). Ultimately, peat subsidence may lead to complete loss of the original peat; exposure of underlying mineral substrate, including acid sulfate soils in many coastal peatland areas (Wösten et al., 1997); and salinization through surface water flooding or saline groundwater intrusion (de Louw et al., 2018), resulting in the loss of land for agriculture.

In their natural state, peatlands can accumulate vertically at a rate of around 0.5–2 mm yr⁻¹ over millennia (Dommain et al., 2014). They also have the capacity to fluctuate vertically in response to seasonal and short-term climatic variations. This ‘bog breathing’ confers resilience to the peatland ecosystem by enabling the ground surface to track water table fluctuations, maintaining wet conditions at the peat surface even during dry periods (e.g., Strack and Waddington, 2007; Dise, 2009; Howie and Hebda, 2018). This capacity of the peat to self-regulate in response to hydrological fluctuations is diminished by drainage, due to changes in peat density, water holding capacity, lateral hydraulic conductivity and connectivity to drainage networks (Howie and Hebda, 2018). Consequently the vertical movement of peat over episodic, seasonal, annual and longer time scales is closely related to the combination of climatic and management pressures to which the peat is exposed.

Evidence that peat vertical motion is related to climate and management raises the possibility that it could be used as an effective, and easily measured, proxy for key metrics of peat condition such as water table depth (WTD) and carbon balance, as well as a tool for evaluating restoration outcomes. A number of recent studies have also suggested that this surface motion can be detected remotely using Interferometric Synthetic Aperture Radar (InSAR) data from satellites such as the European Space Agency’s Sentinel-1 mission, and the Japan Aerospace Exploration Agency’s Advanced Land Observation Satellite-1 (ALOS-1) (Alshammari et al., 2018; Fiaschi et al., 2019;

Marshall et al., 2018; Susanti and Anjasmara, 2019; Zhou et al., 2019; Hoyt et al., 2020). This approach offers clear advantages in terms of the cost, spatial scale and frequency at which information can be obtained, especially for large and remote peatland areas. However, while promising, the use of InSAR as a peatland monitoring tool urgently requires ground validation data, in the form of spatially distributed, high vertical and temporal resolution measurements of peat surface motion.

Despite the societal significance of peat subsidence, and the potential to use vertical peat motion as a proxy for key measures of peat condition and function, records of peat vertical movement are remarkably sparse. Most of the available records are obtained from subsidence poles, which are anchored into the underlying mineral substrate with elevation changes recorded manually, and often infrequently (quarterly or longer). Even these records are sparse in many regions; for example the United Kingdom has a single subsidence pole, the Holme Post, at which a total of 4 m of subsidence has been recorded by periodic measurements made since the original drainage of the site in 1850 (Hutchinson, 1980). Similarly long but isolated records exist for Florida (Stephens et al., 1984) and the San Joaquin delta in California (Deverel and Leighton, 2010). In Southeast Asia, subsidence poles are more widely used, but cover shorter time periods; for example Evans et al. (2019) analyzed subsidence data from over 300 poles deployed across the plantation and forest concessions of one large company, spanning a ten year period. While such records are valuable for determining long-term rates and trajectories of peat subsidence, they reveal little about the short-term (sub-annual) dynamics of peat movement, are labor intensive to maintain, and have a low precision (ca. 1 cm). While it is possible to measure seasonal dynamics of peat surface motion using more frequent measurements of subsidence poles (e.g., Howie and Hebda, 2018; Morton and Heinemeyer, 2019), this approach is labor intensive. As a result, several approaches have been trialled for measuring peat surface elevation change automatically, and with a higher frequency and precision. Zanello et al. (2011) described a system using displacement transducers fixed to a steel tripod, which record movement of aluminum plates resting on the peat surface, with a reported sensitivity of ± 0.125 mm and an hourly frequency. Other potential approaches include the use of sonic or laser distance sensors, mechanical 'float and pulley wheel' systems (Strack et al., 2006), or differential elevation changes recorded by pressure transducers deployed below the water table in paired dipwells that are anchored in underlying substrate and free to move within the peat respectively (Fritz et al., 2008). Challenges for these approaches include mechanical breakdown under the extreme climatic conditions typical of many peatlands (e.g., high/low temperatures, high rainfall, humidity); accumulation of debris on reflector plates required for distance sensors; seasonal snow accumulation in high-latitude systems; and human or animal disturbance. Cost may also be a limiting factor for the use of more sophisticated sensors, restricting their use to well-funded research teams, and constraining the spatial coverage of measurements that can be achieved.

Here, we describe a novel, low-cost, high-precision and high-frequency method for monitoring peat surface motion and water

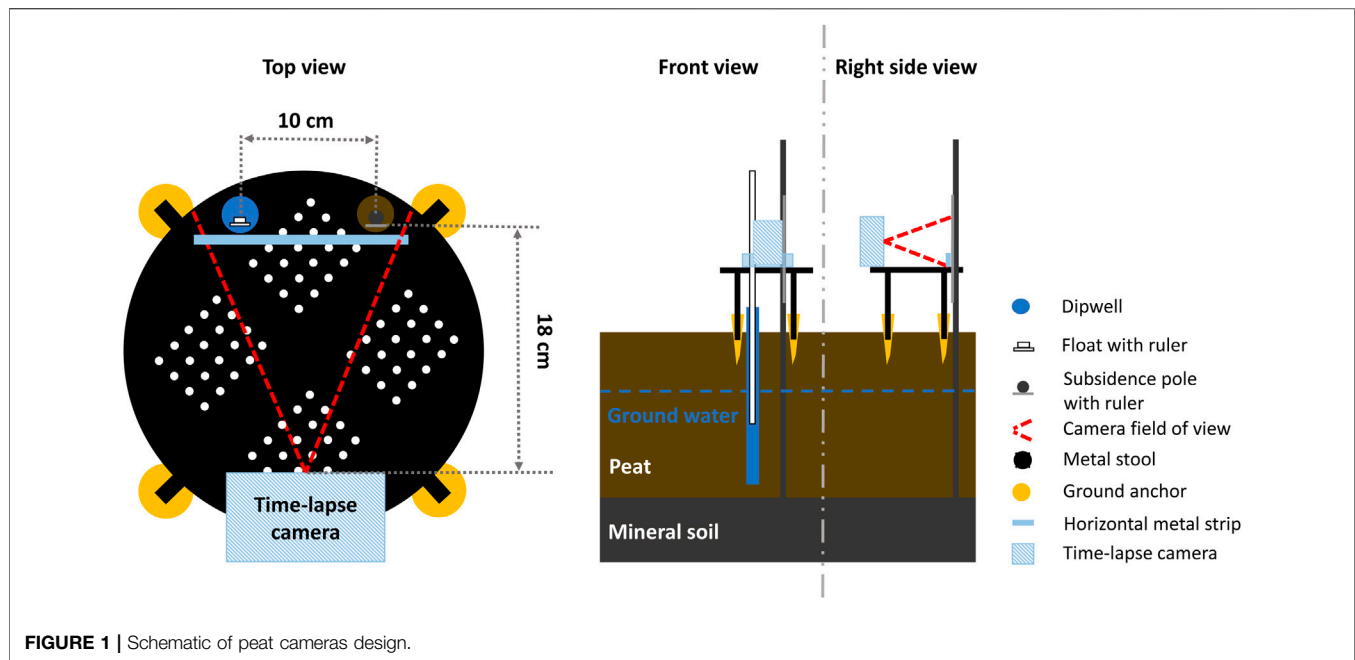
table using cheap and commercially available time-lapse cameras. We describe the system design, the derivation of elevation data from photographic images, and the results of a 2-year deployment of multiple cameras to a range of contrasting peatland sites in Indonesia. We evaluate system robustness and accuracy, compare results against manual subsidence pole and commercial water table logger measurements, and examine the temporal dynamics of peat motion as a function of diurnal, hydrological, seasonal and long-term drivers of change. We also examine the extent to which peat behavior is influenced by land-management, and therefore the potential to use remote sensing of peat motion as a proxy for other peatland functions and properties.

METHODS

Peat Camera Design and Operation

We developed a simple, low-cost (around \$300 per unit) camera-based system to measure small-scale variations in peat surface elevation, along with changes in WTD. This used a commercially available time-lapse camera (Wingscapes Timelapse Cam Pro WCB-00121, Alabaster, Alabama, United States). Similar cameras have been remotely deployed in similar habitats in the region to monitor wildlife populations with high success (e.g., Cheyne et al., 2016). The camera was fixed to a metal stool within a metal housing (to provide some shelter to the camera and security from theft), facing a horizontal metal strip that acted as a measurement level within the photographs (Figures 1, 2). The stool then was placed over a metal subsidence pole that had previously been inserted vertically through the peat into underlying mineral substrate, which acted as a fixed reference level. Approximately 2 m of the pole was left projecting above the peat surface, and a 1 m metal ruler was attached to this such that the mid-point of the ruler was at the level of the camera lens. The subsidence pole passed through a pre-cut hole in the stool at a distance of 18 cm from the camera lens, behind the metal strip. The stool was then attached to the peat surface using ground screws attached to each leg of the stool, which were adjusted until the stool top and camera were horizontal. The stool and camera thus moved with the peat surface, and took photographs of the meter ruler on the fixed subsidence pole. For flood-prone sites the stool legs were extended to provide greater ground clearance.

To measure changes in WTD, we installed a dipwell comprised of a perforated, 7.5 cm diameter \times 2.5 m long plastic pipe with a sealed base into the peat adjacent to the subsidence pole. Water level inside the dipwell was measured by means of a plastic fishing float of slightly smaller diameter than the dipwell, attached to a lightweight aluminum pole with a measurement scale attached, which passed through a second hole at a distance of 10 cm from the subsidence pole, and within the field of view of the camera. After initial trials, the float and pole were found to rotate within the dipwell, making the depth difficult to read. The design was refined by attaching a lightweight flexible PVC fibreglass tape measure to a U-channel aluminum wiggle wire (15 \times 25 mm), and passing the U-channel and tape measure through a rectangular hole in a metal plate attached to the stool top. Although the



dipwell was open, to allow the float and the pole to move freely, the stool and the metal plate on top of it acted as a protection against debris and limited rainwater ingress.

The time-lapse camera was programmed to take photographs several times per day, initially at a 3 h frequency. This was changed to an hourly frequency in late February 2020 to enable a detailed assessment of system capability for monitoring change in WTD. To improve night-time imagery, we covered the camera's flash with partially transparent tape to reduce glare from the ruler so that the scale was readable. By taking multiple photographs during each day, we were able to record rapid or diurnal fluctuations in peat elevation and water table, and also ensured that at least one good image was usually obtained during periods of rainfall, when raindrops sometimes caused image blurring.

The cameras were powered by six C-cell alkaline batteries. Camera images were stored to a 32 Gb SD card, which could either be swapped during site visits or downloaded *in situ* via a USB cable. Cameras were typically left to run in the field for a period of one to three months between downloads, to minimize site disturbance, while not risking long periods of undetected equipment malfunction, damage or theft that could occur with less frequent checks.

Study Sites

To date, approximately 50 peat cameras have been installed on tropical peatlands in Central Kalimantan and Sumatra, Indonesia, and in Sarawak and North Selangor, Malaysia; at a range of temperate peatland sites in the United Kingdom; and on a boreal mire in Sweden. Here, we report the first results, spanning two wet and dry seasons, from eight sites in Central Kalimantan (**Table 1**; **Figures 2, 3**). All cameras were located within established field research sites operated by the University

of Palangka Raya as part of the United Kingdom Global Challenges Response Fund SUSTAINPEAT project. All sites are located between the Sebangau and Kahayan Rivers to the north and south of the city of Palangka Raya (from latitude 1.88°–2.35°S, longitude 113.47°–114.10°E). The area south of Palangka Raya was heavily deforested and drained via a network of canals in the 1990s as part of the failed Mega Rice Project, since then it has been subject to severe and repeated fires (Page et al., 2002). The area now comprises fragments of secondary forest, large areas of smallholder agriculture, smallholder and some larger oil palm plantations, and extensive areas of degraded shrubland dominated by ferns, regenerating native trees and non-native *Acacia mangium* (Page et al., 2009). In this area we deployed six cameras: two in smallholder agricultural land, one in a smallholder oil palm plantation, one in secondary forest and two in burned shrubland. The area north of Palangka Raya includes areas of more extensive forest, with some smallholder agriculture and smaller oil palm plantations. This area is in general less drained than the southern area, and fires are less frequent. Here we installed two cameras: one in a smallholder oil palm plantation, and one in secondary forest.

The study region has an average annual temperature of 26°C, with little seasonal variation, and a mean rainfall of 2,500 mm yr⁻¹ (Hirano et al., 2012). Rainfall is strongly seasonal with a wet season from November to April and a dry season from around June to September, though this may extend into and beyond October in drought years (**Figure 4**). The severe El Niño related dry season of 2015 led to widespread fires, following which the Indonesian Peat Restoration Agency (Badan Restorasi Gambut, BRG) was created, and instituted a program to restore degraded peatlands and raise water levels through the installation of dams on canals. However another positive El Niño phase in 2019



FIGURE 2 | Peat cameras installed at four sites in Central Kalimantan (clockwise from top left: Forest, oil palm plantation, smallholder agriculture, previously burned scrubland).

TABLE 1 | Locations, properties and management histories of Central Kalimantan study sites.

Name	Latitude	Longitude	Peat depth (cm)	Bulk density (g cm^{-3})	Management history
Oil palm, misik	-2.3001	114.0308	373–392	0.25 ± 0.01	Opened in 2015 after fire, 30 m from main drainage
Oil palm, hampangan	-1.9199	113.578	342–350	0.18 ± 0.01	Affected by fire in 2007, water levels maintained by ditches and dams
Agriculture, kalamangan	-2.28952	114.0134	365–377	0.24 ± 0.01	Opened in 1980s, 35 m from main drainage, irrigated in dry season
Agriculture, misik	-2.3048	114.028	292–300	0.26 ± 0.01	Opened in 2015 (after fire), 220 m from main drainage
Burned Area, RePeat	-2.3370	114.0704	267–277	Not determined	Shrub, severely affected by fire in 2015. Part of 'RePeat' rehabilitation project
Burned Area, south	-2.35411	114.0959	250–300	Not determined	Shrub, affected by fire in 2015
Forest, UPR	-1.8845	113.4733	83–90	0.08 ± 0.01	Secondary forest, affected by fire in 1997
Forest, KHDTK	-2.3527	114.0923	226–284	0.14 ± 0.01	Secondary forest, affected by fire in 1997

resulted in a prolonged dry season, severe water table drawdown in some areas (up to 2 m) and a recurrence of fires in many areas.

The 2020 dry season was shorter and wetter than average, and few fires occurred, as La Niña conditions developed.

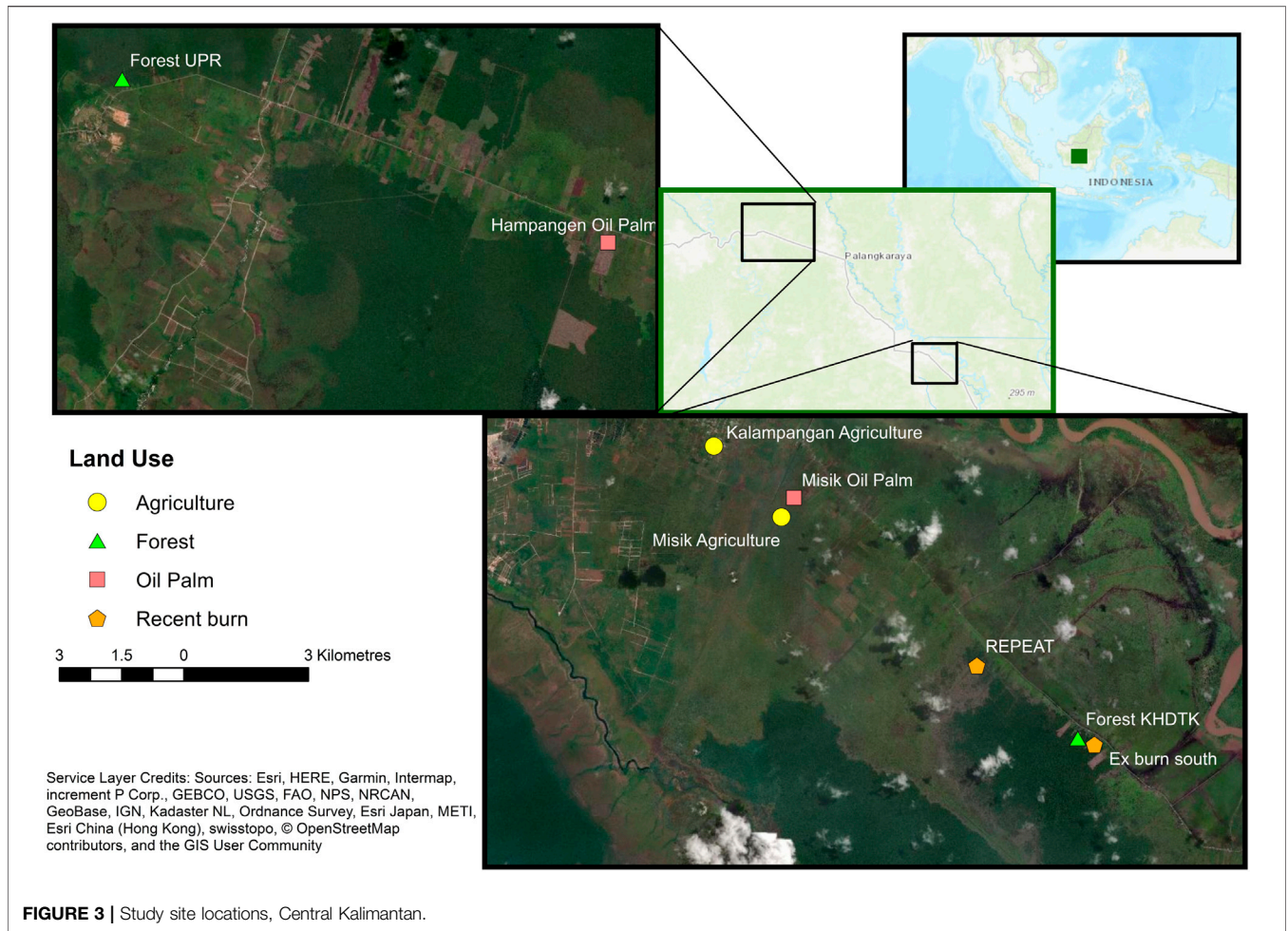


FIGURE 3 | Study site locations, Central Kalimantan.

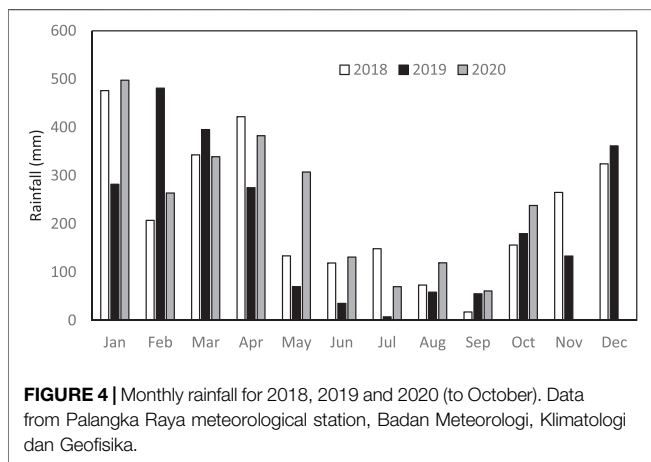


FIGURE 4 | Monthly rainfall for 2018, 2019 and 2020 (to October). Data from Palangka Raya meteorological station, Badan Meteorologi, Klimatologi dan Geofisika.

Test Data Collection

To evaluate instrument performance, a set of 6–10 metal and PVC poles were installed in areas near the camera site, at which subsidence was recorded manually on up to nine occasions during the measurement period, by measuring the distance from the top of the pole to the peat surface (see e.g., Evans

et al., 2019). Metal poles were considered likely to be more robust in the actively managed and dynamic landscapes being studied, while PVC poles were installed to check for any sinking of the heavier metal poles into the underlying substrate. As no such sinking was detected during the period of measurement, data from both sets of poles were pooled. To compare camera and manual subsidence data we derived a mean of manual elevation values for each time point, and the mean camera-derived elevation value for the same day. Change in elevation was then calculated relative to a zero datum on the day of the first manual measurement at each location.

Manual subsidence poles were distributed near the camera sites, along transects or grids at a spacing of around 50–100 m, with the intention of measuring variations in subsidence within the surrounding area, rather than specifically for testing camera performance. However in most cases subsidence was found to be fairly consistent at this scale, enabling a comparison to be made. An exception was the Kalamangan agricultural site, where we included poles installed within the farm itself, but excluded four poles located in neighboring scrubland that were affected by fire during the study period. We also excluded manual poles with incomplete data, as well as poles that suffered visible disturbance during the study period as a result of land-management activities.

To test the camera-derived water table measurements we ran cameras at three sites (Misik Oil Palm, RePeat Burned site, UPR Forest) alongside DipperLog Nano pressure transducers (Heron Instruments, Ontario, Canada) installed in adjacent dipwells. Both instruments were set to record at an hourly frequency. The period of parallel measurements ran from February 21st to June 30th 2020. A DipperLog Nano was also operated at the Hampangen Oil Palm site for the duration of the study. As no water table loggers were operational at any of the southern sites for the first part of 2019 we also obtained water table data collected by the Japanese Science and Technology Agency and Japan International Cooperation Agency “Wild fire and carbon management in peat-forest in Indonesia” project (Takashi Hirano, pers. comm.) located in burned scrubland close to the RePeat Burned site. These data were used to indicate the general pattern of variation in WTD in this area.

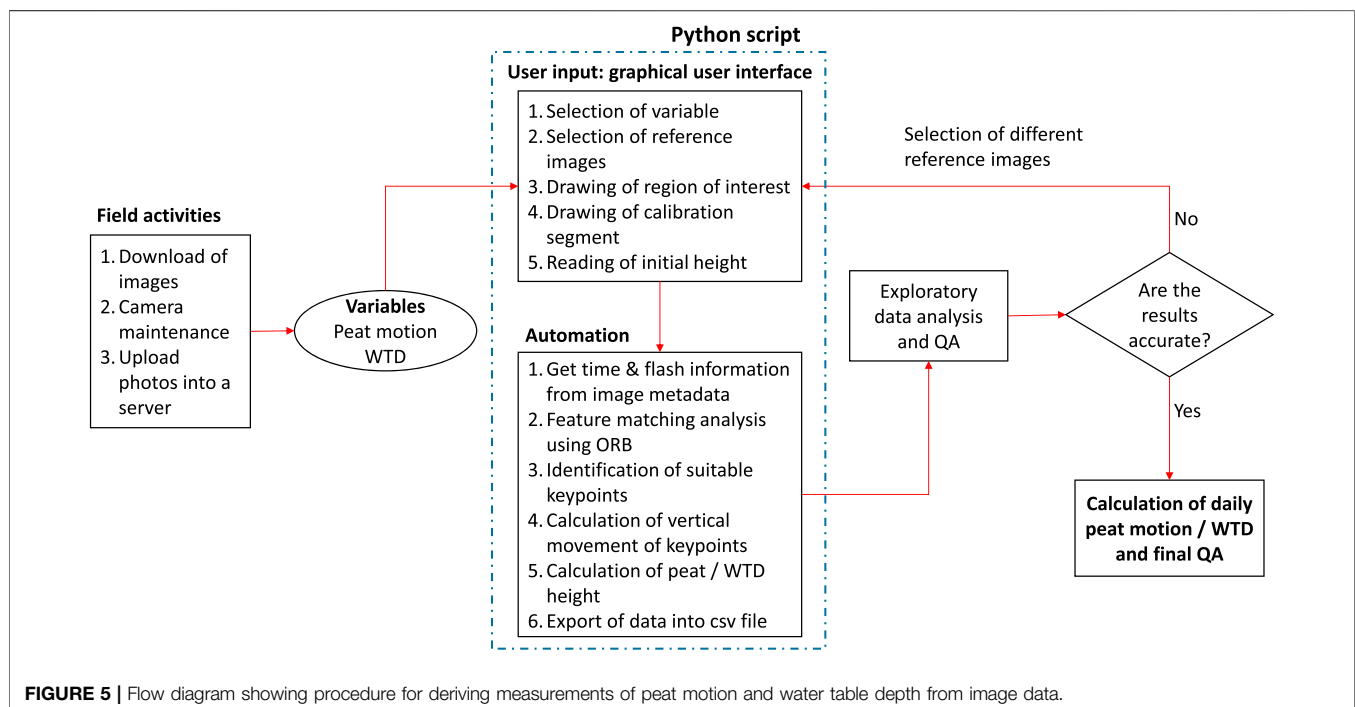
Data Analysis

Images were processed using a custom written *Python* script via a graphical user interface (Figure 5). Although the script automated the peat height data extraction, it also required some initial parameters that had to be manually provided by the user. After an initial visual assessment of the images to be processed, the most representative image, based on light conditions and the ruler numbers shown on the images, was used as a reference. Images taken at night and during the day, as determined by whether the flash was used, were processed separately, as lighting conditions were too different for processing together. Therefore, the reference image was selected separately for day and night images. Thereafter, an initial height reading (manually read from the ruler in the

image) and calibration (line segment drawn on the image and given a measure in centimetres, usually 1 cm) was recorded from the reference images. In addition, a region of interest was manually selected around the ruler. This region of interest defined the area of each image containing the points of interest with distinct features, or keypoints. The defined area was effectively cropped, and compared with the same cropped area from the reference images. Keypoints were characterized by their coordinates, orientation and scale. By positioning the area of interest near the middle of each image, distortion toward the edge of the image was minimized, and selection of keypoints along the ruler both above and below the center meant that any minor distortion within the area of interest was effectively canceled out.

Each cropped image underwent feature matching analysis using the ORB method (Rublee et al., 2011) to locate keypoints. ORB (Oriented FAST and rotated BRIEF) is an open source script which combines two methods, FAST (Features from Accelerated Segment Test) and BRIEF (Binary Robust Independent Elementary Features), where FAST describes the methods of detecting where a feature is and BRIEF is a method for reducing the memory required to store and process all the relevant vectors produced. FAST locates features essentially by detecting corners. For each pixel it evaluates a circular radius of pixels around that pixel and compares their intensity (how light or dark they are) to a threshold intensity difference, starting with opposite orthogonal points around that circle and then continuing round the circle if they are brighter or darker. A feature is detected if there are a significant number of contiguous pixels in that circle that are brighter or darker than the central pixel.

Keypoints in each image (i.e., distinct features identified by ORB as described above) were paired to those found in the



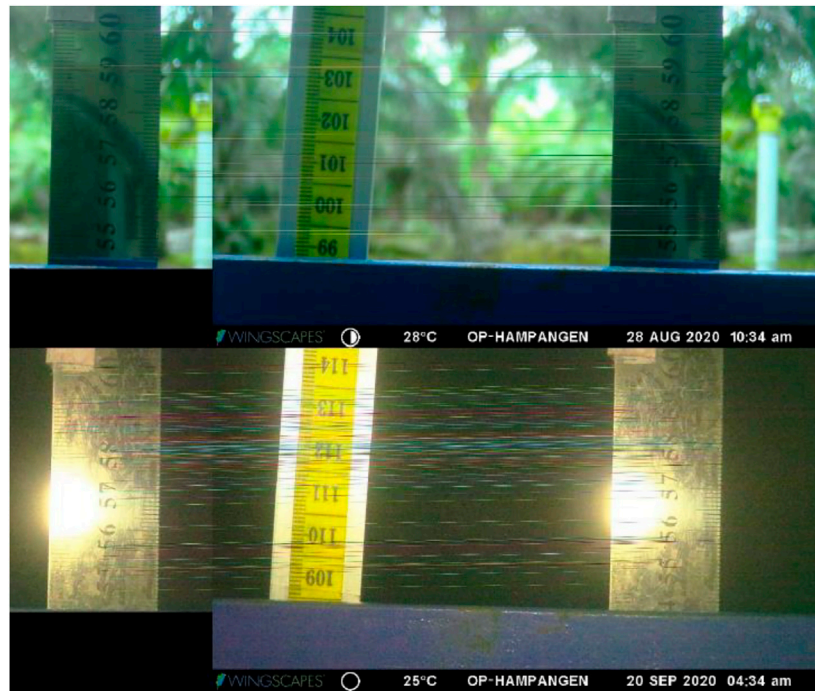


FIGURE 6 | Examples of image processing for daytime and night-time images at the Hampangen Oil Palm site. Ruler in image on right is compared to reference image on left, containing the cropped region of interest with potential keypoints (central scale is the water table gauge). Colored lines represent individual matches between keypoints, which are used to calculate vertical displacement.

reference image using a ‘brute force’ matcher which compares each keypoint against every keypoint in the reference image to find pairs of keypoints. The pixel locations of each keypoint pair were compared to get a movement vector in pixels. Any pairs that did not have similar vectors (within 1 pixel and 1°) to other pairs from the same image were discarded, and images were required to have at least two matched pairs of keypoints with similar vectors. Only the vertical component of each movement vector was used in analysis as in theory only vertical movements should be possible, however horizontal movements were used to flag anomalous movements. The vertical movement of suitable keypoints from the reference image was converted to movement in cm using a manually provided calibration value based on the number of pixels per cm in the images, and then converted to a height measurement by applying the difference to the manually read measure on the reference image. Images that could not be automatically processed by the script were then manually read by the user, sufficient to obtain at least one elevation value per day. At the end of the automation process, the script exported all the data into a csv file. This file contained the photo id, the date and time, a code identifying if it was a day or a night image, the average vertical movement (in pixels), the average angle change, the number of suitable keypoints, the calculated height (in cm) and a warning message if any horizontal movement was detected. All peat height measurements recorded within each day (either at hourly or 3 hourly intervals) were averaged to obtained daily values. When gaps of no more than 5 days occurred due to system

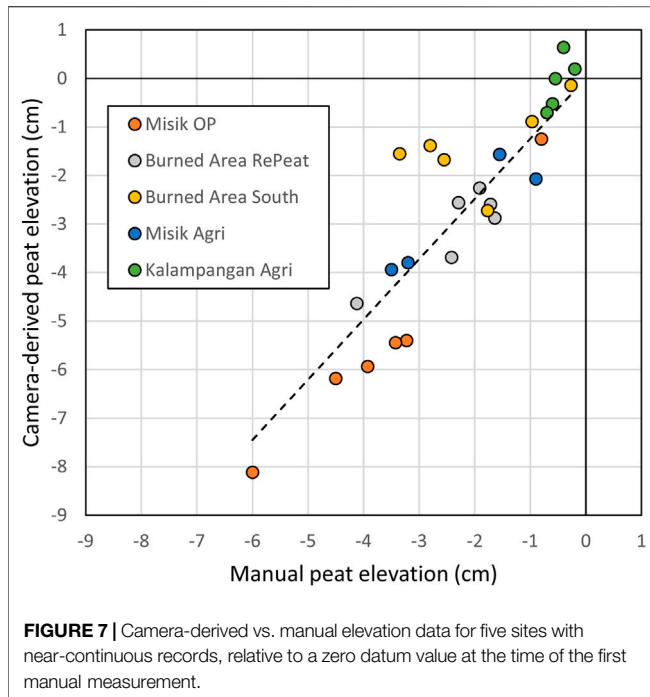
malfunctioning or adverse weather conditions, peat height values were estimated by linear interpolation. Longer gaps were left blank.

The eight Kalimantan monitoring sites provided sufficient data to calculate annual subsidence in 2019. To reduce the effect of short-term hydrologically driven fluctuations we calculated annual net subsidence as the change in peat elevation observed between the first two weeks of January 2019, and the first two weeks of January 2020. At two sites with missing data during one of these time periods, we used the closest available two week period. Although this could introduce an error in the calculation, the December-February period is the wettest part of the year, so relatively little subsidence occurs at this time, and the magnitude of any error is therefore expected to be small.

RESULTS

Image Processing

In general, the image processing method worked well for deriving peat motion data. **Figure 6** shows example of daytime and night-time image matches. Image quality tended to be best at sites with sparse vegetation (fields, plantations and bare ground) where there was little vegetation interference in the field of view, and where humidity was lower. Vegetation interference occurred more often at forest sites, for example due to creeper growth up the instrumentation, which required periodic maintenance. The feature analysis was able to detect keypoints with a modest



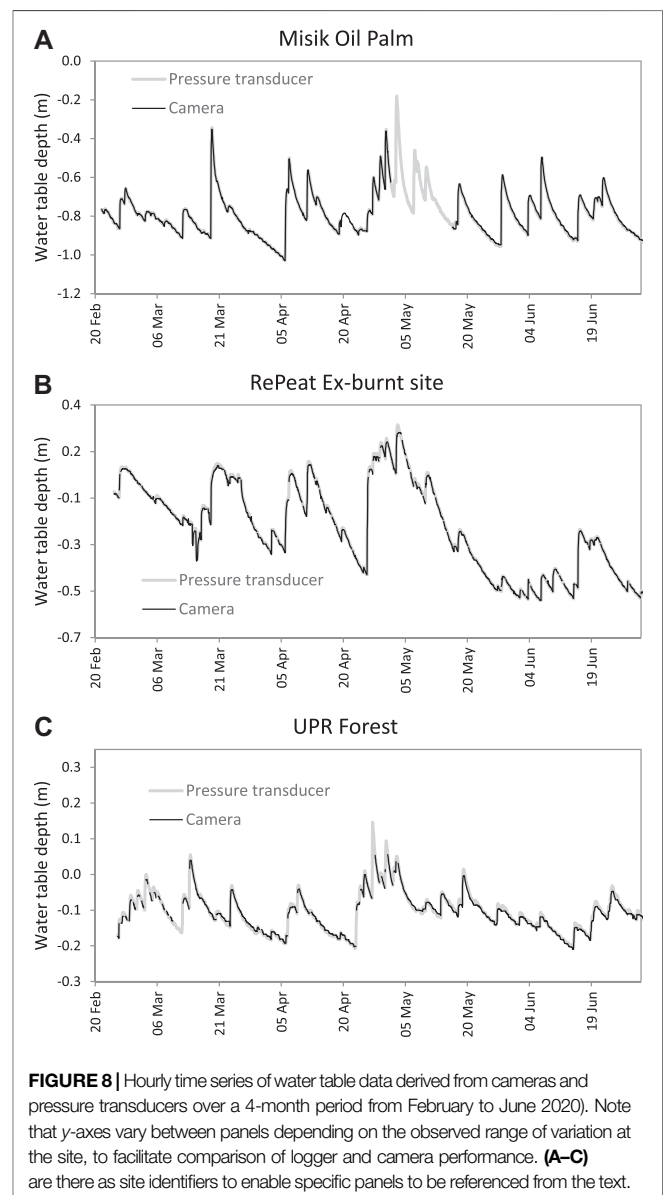
level of image blurring, but not when blurring was more severe such as during and immediately after rain events. Since these events are typically of short duration in the study area, we were generally able to process at least one image per day. The use of a standard meter ruler provided some non-unique features in the image (e.g., repetition of ‘3’ in the 30, 31 and 32 cm labels) but in a clear image the software was usually able to correctly identify five or more keypoints. Although performance was often similar for daytime and night-time images, at some specific sites, night images showed a better performance (i.e., larger number of identified keypoints, e.g. 100 or more); provided that the opacity of the tape over the flash was sufficient to avoid image burnout and not too dark to negate the effect of the flash. In many cases where the image detection software was unable to identify keypoints, we were able to identify these manually. All images were manually checked for clearly erroneous matches, which were then corrected when numbers were clearly visible. Success rates of image processing using the script varied between 45 and 98% depending on the site and the collection period. Precision of automatically classified measurements was sub-mm (the script was able to detect vertical movements of a single pixel, which was equivalent to 0.03–0.04 mm), while precision of manually processed data, when the value was read directly from the ruler, was around 1 mm (i.e., the smallest subdivision of the ruler).

Processing water level data from the images was in general more problematic, due to the larger range of vertical movement (up to 50 cm in 3 h in response to rainfall at some drained sites). This meant that the entire section of the measurement scale visible in one image could move out of the field of view of the camera by the time of the next image, such that no matching

keypoints could be obtained. Image processing through the script resulted in success rates of around 20% and therefore, to extract water level data it was necessary to process the remaining images manually. All images were visually checked to manually correct mismatched keypoints and erroneous extracted water level data. Precision was around 1 mm.

System Performance

Of the eight cameras installed, five provided near-continuous records of surface elevation change over the study period, while the other three provided partial data, sufficient to derive total subsidence over the year. Data loss at the Hampangen Oil Palm site occurred as a result of a programming error with the camera, resulting in only sporadic measurements from april to October 2019. Periods of data loss at the forest sites resulted from camera failure due to moisture ingress (typically leading to the camera to



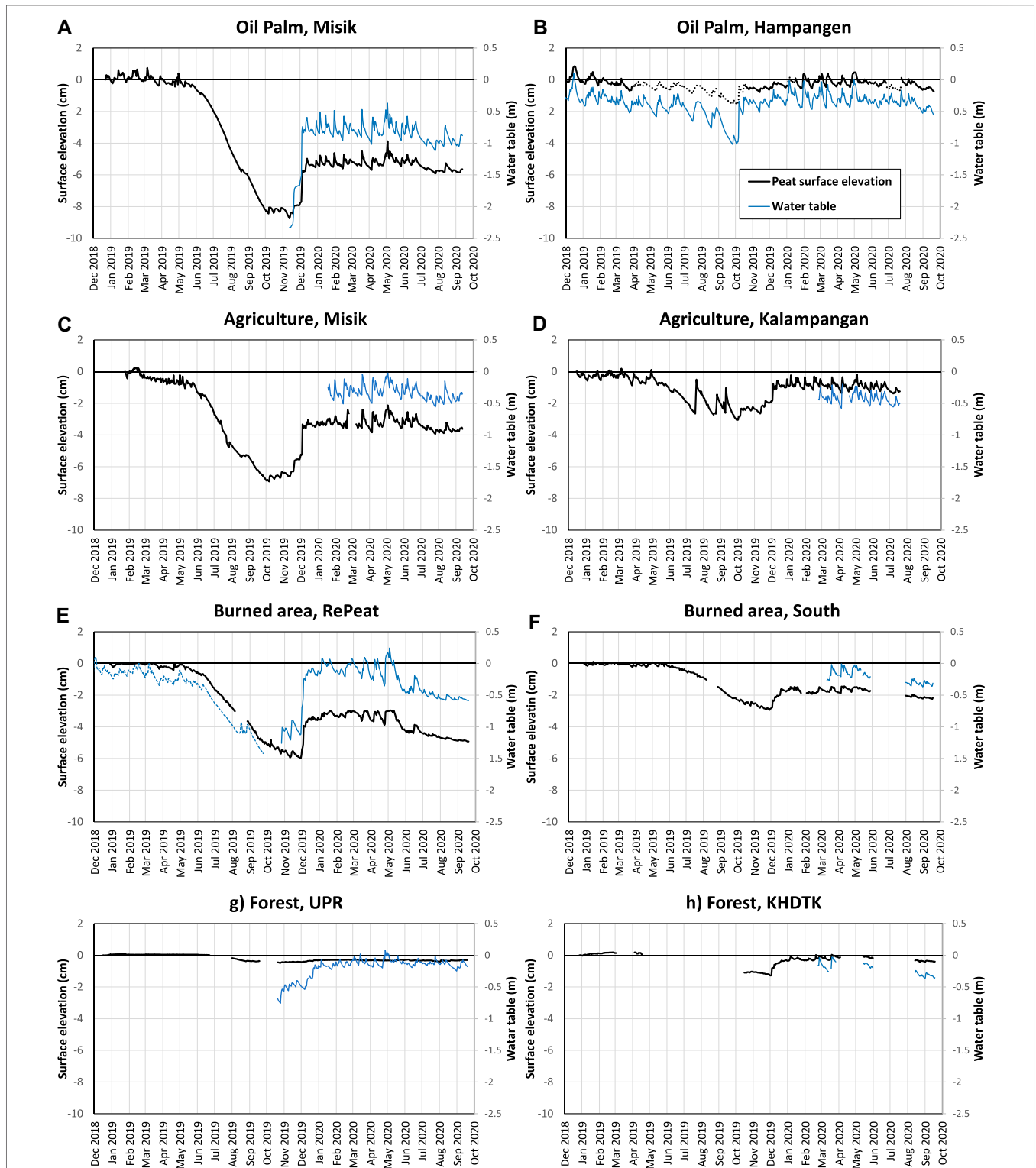


FIGURE 9 | Time series of peat elevation (black, left y-axis) and water table depth (blue, right y-axis) over the full measurement period. All data are plotted on the same y-axis scales to facilitate comparison. The black dashed line at Hampangen Oil Palm indicates data that were gap-filled using WTD data and the blue dashed line at RePeat shows WTD data obtained from a pressure transducer operated nearby (see text for details). **(A–H)** are there as site identifiers to enable specific panels to be referenced from the text.

TABLE 2 | Annual net subsidence for 2019 for the Kalimantan sites.

Type	Location	Subsidence (cm)
Oil palm	Misik	-5.27
Oil palm	Hampangan	-0.36
Agriculture	Misik	-3.21
Agriculture	Kalampangan	-0.40
Burned area	RePeat	-3.17
Burned area	South	-1.50
Forest	UPR	-0.30
Forest	KHDTK	-0.26

taking photos at random intervals, usually every few seconds, or stopping completely, likely due to an electric short-circuit). This problem appears to have been more acute in the forest sites due to extremely high humidity under the forest canopy. Lens fogging also occurred in moisture-affected cameras, while on one occasion, ants were found inside a camera which also resulted in system malfunction. These problems were addressed by taping over the seals on the camera, and by providing protection from rain. Moisture-affected cameras were generally found to recover if removed from the field and dried.

At the two burned sites, we temporarily removed the cameras (poles and platforms were left in place) during August 2019 due to the risk of them being destroyed by fires that were active nearby at the time, although neither site ultimately burned. For the five sites with near-continuous camera data, a comparison of camera-derived and manual elevation change (Δ Elevation, i.e., change relative to the site datum value) is shown in **Figure 7**. A linear regression through all measurements (and excluding the 0,0 values for all sites) gave the relationship:

$$\Delta\text{Elevation (camera)} = 1.295 \times \Delta\text{Elevation (manual)} \text{ Adjusted } R^2 = 0.916, p < 0.001, n = 28.$$

The coefficient above 1.0 suggests that the cameras might be slightly over-estimating Δ Elevation, although this deviation was not observed at all sites. The Misik Oil Palm site exerts a particularly strong influence; without data from this site the regression coefficient would be 1.14. At this site, the camera was located 30 m from a drainage ditch, whereas most manual poles were further away; simultaneous manual measurements of WTD on three occasions suggested that the camera site had considerably deeper drainage (mean WTD -0.75 cm) compared to the subsidence pole locations (mean WTD -0.54 m). Thus, differences between camera and manual Δ Elevation values at this site may represent real differences between the sites, rather than measurement artifacts, although clearly the behavior of camera and manual sites was highly correlated ($R^2 = 0.97, p < 0.001$).

We compared WTD data obtained from the cameras with those from pressure transducers at three sites, for the period February to June 2020 (**Figure 8**). The Misik Oil Palm logger experienced one extended period of data loss due to a palm frond falling on top of the dipwell. In addition, several shorter periods of data loss occurred at the UPR Forest site when firstly the tape covering the flash was too dark and secondly, when the camera float apparently jammed, notably at very high water levels (>5 cm above the surface) when the float may have jammed against the stool. At this site, it was also often difficult to obtain useable

images during rain events, evident in **Figure 8C** as gaps on the rising limb of a number of event hydrographs. For the remainder of the time, however, all three sites showed remarkable correspondence between the two sets of measurements (Misik Oil Palm: $\text{WTD}_{\text{camera}} = 0.997 \text{ WTD}_{\text{pressure transducer}}$, $R^2 = 0.986$; RePeat Burned: $\text{WTD}_{\text{camera}} = 0.997 \text{ WTD}_{\text{pressure transducer}}$, $R^2 = 0.999$; UPR Forest: $\text{WTD}_{\text{camera}} = 0.953 \text{ WTD}_{\text{pressure transducer}}$, $R^2 = 0.994$; all $p < 0.001$). The camera-derived data therefore appear to be of similar quality to the pressure transducer data.

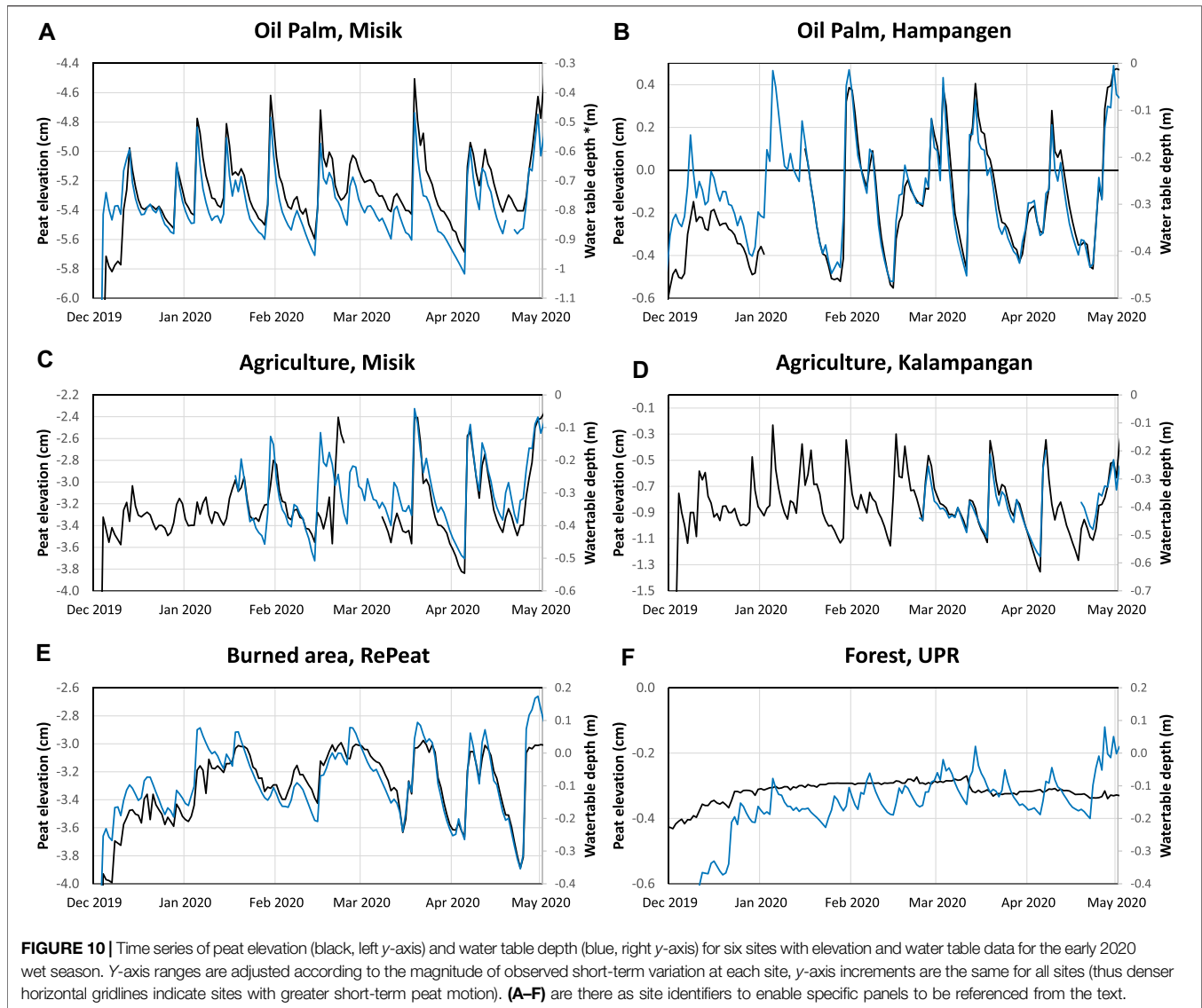
Peat Elevation and Water Table Time Series

Measured elevation changes for all sites are shown in **Figure 9**. The data span two wet seasons and two dry seasons, but the 2019 dry season was notably drier than 2020. As noted above, there were substantial data gaps at the Hampangan Oil Palm site and the two forest sites in 2019. At Hampangan, where a pressure transducer was in operation throughout the study, we observed a strong linear relationship between peat elevation and WTD during periods of camera operation ($R^2 = 0.83, p < 0.001$) so this was used to gap-fill the elevation record (dashed line in **Figure 9**). The gap-filled record aligns well with two brief periods of camera operation during this time, providing some support for this approach, however derived peat elevation changes during this gap-filled period are uncertain.

More generally, the elevation data demonstrate high overall coherence among sites. All sites showed stability or slight subsidence during the wet season at the start of 2019, followed by sustained subsidence during the severe dry season, which continued until the end of November 2019. All sites then rebounded rapidly, coincident with a rapid recovery in the water table where this was measured. At some sites, rebound was complete (i.e., peat elevations returned to where they had been in early 2019) but in others it was partial, despite water tables returning to close to the surface in some cases. The less severe 2020 dry season was associated with much less water level drawdown, and at most sites the peat surface remained stable, although there was evidence of renewed subsidence at some sites, including both Misik sites, and the RePeat Burned site. At the RePeat site, a canal was dug close to the camera in around April 2020, which likely accounts for the accelerated subsidence here relative to other locations.

Annual Subsidence and Effects of Land-Use

We were able to estimate annual net subsidence from camera data for the 2019 calendar year at all sites. Observed values (**Table 2**) ranged from -0.3 cm at the two forest sites (where a negative value indicates a decline in the ground surface) to -5.27 cm at the Misik Oil Palm site. Net accumulation did not occur at any site. As is evident from **Figure 9**, peat elevations declined by more than this amount at the peak of the 2019 dry season, then partly recovered. The relative stability of peat elevations during the wet January-April periods in both 2019 and 2020, when hydrological conditions were similar, suggests that the net change between these two periods represented long-term subsidence (i.e., peat oxidation and compaction) rather than a short-term shrink-swell response to drying and re-wetting.



At this stage, we do not have sufficient data to estimate annual WTD, which previous studies have shown to be a strong predictor of subsidence rate (e.g., Hooijer et al., 2012; Evans et al., 2019). However from the limited data available it is clear that sites with uncontrolled deep drainage during the dry season (e.g., Misik Oil Palm, where the water table was >2 m below the surface when measurements began in November 2019, and the RePeat Burned site where it was >1 m) experienced relatively high subsidence, whereas sites where water levels remained higher (e.g., UPR Forest, Hampangen Oil Palm) experienced far less subsidence. These relationships partly tracked land-use; the forest sites both showed very limited motion during periods when the cameras were operating, and negligible annual subsidence. The greatest peat shrinkage during the 2019 dry season, and largest annual net subsidence, occurred at the intensively managed and deeply drained Misik Oil Palm and agricultural sites. The two partly drained but unmanaged former burned sites were intermediate between these two extremes,

although it is notable that peat elevation at the burned sites (especially RePeat) appears to have decreased again during the less intense 2020 dry season, whereas most other sites remained relatively stable.

Two sites did not behave as expected based on their land-use. The Hampangen Oil Palm plantation showed negligible overall subsidence during the measurement period, despite active plantation management. This site, which is located in the poorly drained area north of Palangka Raya, had much higher water tables than the agricultural sites to the south: apart from a brief period during the peak of the 2019 dry season, water tables were always within 50 cm of the peat surface, and frequently higher. While the camera was not operational during much of the 2019 dry season, gap-filled data based on a correlation with water table (Figure 9) suggest that maximum shrinkage may have been less than 2 cm, whereas it exceeded 8 cm at the deep-drained Misik Oil Palm site. The recovery of the peat surface by January 2020, to approximately the same level recorded in January 2019,

suggests that these relatively wet conditions, which are unusual for oil palm cultivation, may have been sufficient to minimize subsidence.

The Kalamangan Agricultural site also diverged strongly from the behavior of the other agricultural site at Misik, despite their close proximity (2.5 km apart) and apparently similar drainage (both sites lie within the same canal network and were observed to have similarly deep water tables during the peak of the 2019 dry season). However, unlike the Misik site, the farm at Kalamangan is periodically surface-irrigated via a borehole that extracts water from the aquifer beneath the peat. The three sharp periods of peat uplift during July–September 2019, which were not associated with rain events, are believed to be due to irrigation of the field containing the camera (A. Jaya, pers. obs.). These irrigation events seem to have played a major role in reducing the degree of peat shrinkage during the dry season (maximum observed shrinkage of 3.0 cm, vs. 7.0 cm at Misik), and in the subsequent wet season the peat recovered almost to its original elevation, whereas it remained 3.2 cm lower at Misik.

Response to Short-Term Hydrological Variation

Figure 10 shows camera-derived peat elevation and water table data for the wet season at the start of 2020, for the six sites with relatively complete data during this period. It is clear that, in almost all cases, peat elevation tracks WTD very closely. This occurs despite marked differences in hydrological conditions at different sites. For example at the Misik Oil Palm site, with efficient drainage, water levels repeatedly rose by around 0.4 m in response to rain events, before rapidly declining until the next rain event. This pattern was replicated in the elevation data, with an amplitude of around 0.8–1 cm. At the Hampangen Oil Palm site, despite much higher water levels, the amplitude of both water level change and peat elevation change between wet and dry periods was the same. The two agricultural sites also had similar amplitudes of short-term variation in response to rain events. The burned site showed a more subdued hydrological response, which was also reflected in the peat motion. The forest site has the smallest water table fluctuations in response to rainfall, typically <0.2 m. Here, in contrast to all other sites, we observed negligible peat elevation variation in response to short-term rain events, although there was some steady upward movement of the peat in December 2019, during the transition from dry to wet season.

At the managed sites, there was very little indication of hysteresis in the response of peat elevation to water table change; i.e. water table and peat elevation rose and fell more or less simultaneously. At the burned site, some peaks in peat elevation were slightly lagged behind peaks in water table, but in other cases no hysteresis was evident.

DISCUSSION

System Performance and Refinement

Given the simplicity and low cost of the camera-based system compared to current commercially available sensors, our results

were highly encouraging, and enabled observation of aspects of peat behavior that were not previously detectable, as discussed below. The two main challenges for the camera method are reliability in the field, and data processing.

Field data loss occurred for a number of reasons. One was simply miss-programming of the cameras, for example by setting time intervals to seconds rather than hours. This problem was resolved as instructions were made clearer and operators became more experienced. Adjusting the strength of the camera flash (using semi-opaque tape) reduced issues of image burnout or under-exposure at night, increasing the number of usable images obtained per day. Other causes of data loss were image blurring by raindrops on the lens, incorrect camera focus, water ingress into the camera (particularly in high-humidity forests) and blocking of the camera view by growing or falling vegetation. Refinements to system design made during the study included better waterproofing of the camera, and addition of a roof over the camera, which reduced data loss due to rain and falling debris. Some water ingress to the open dipwell likely still occurred, but the near-1:1 correlation with data obtained from pressure transducers in adjacent capped dipwells suggests that this had a negligible impact on results. The lateral hydraulic conductivity of tropical peat is typically high (Evans et al., 2014), which may have limited the extent to which rainwater could accumulate in the dipwell above the water table. In peat with a lower hydraulic conductivity, such as high-latitude bogs, more issues with rain ingress are possible. We plan to reduce this issue in future refinements of the system by adding a PVC cap to the dipwell with a narrow hole through which the float device can move freely.

At another trial site in Malaysia, one camera was damaged by wild boar, but as this problem did not arise elsewhere we did not place the cameras inside enclosures, to avoid ground disturbance. Periodic visits to remove debris and ground vegetation, and to conduct general checks of the equipment and its functioning, generally minimized data loss and are therefore recommended, irrespective of limits imposed by battery life and SD card capacity. However in future we aim to develop a system with telemetry and off-grid power to provide an immediate indication of problems, enabling more efficient operation, and to reduce the need to access the camera to download data and change batteries, thereby minimizing disturbance issues.

The main additional challenge for the water table loggers was jamming of the float system, either within the dipwell or as it passed through the stool. These problems were reduced by using a smaller float relative to the diameter of the dipwell, removing any rough edges inside the dipwell (e.g., those created by drilling holes), and passing the pole and ruler through a metal plate on the stool to minimize friction and ensure that the ruler was correctly oriented toward the camera. The stool itself provided protection against debris ingress into the dipwell, and the addition of a PVC cap in future should further reduce this issue.

Data processing represented a significant challenge. For peat elevation, the image processing software worked well, although some manual error-correction and image matching was generally needed. Processing the water table data was more problematic, because the vertical movements were often too large to allow keypoint pairs to be identified. The use of a standard meter ruler

also presented challenges for identifying unique keypoints, which might partly be overcome through the use of a purpose-built scale, e.g., using unique symbols and colors.

Despite the data processing challenges, the cameras produced water table data that were almost identical to those obtained from commercial pressure transducers, with no evidence of any systematic bias (R^2 and gradient of relationships between the two methods both close to 1; **Figure 8**). The cameras also provided highly precise measurements of change in peat elevation, and could detect movements of less than 1 mm with very little short-term noise. Where small fluctuations were observed during sequential measurements, these were found to be consistent from day to day, and to track diurnal variations in WTD associated with daytime evapotranspiration. While we have not yet been able to precisely quantify measurement error, the method appears to compare well with the dual pressure transducer method of Fritz et al. (2008) (reported standard error ± 2 mm), and is clearly superior to acoustic sensors with a reported precision of ± 1 cm (e.g., Campbell SR50A).

The comparison of camera-derived data with manual subsidence pole data (**Figure 7**) indicated that the cameras are able to accurately capture sustained changes in peat surface elevation over time. The subsidence poles were installed to capture local variability rather than with the specific aim of testing camera performance, and were therefore in some cases 100 m or more away from the camera site, which likely contributed to some scatter in the relationship. We also often found weaker coherence in temporal behavior among subsidence poles located in the same area than we did between cameras at different locations, suggesting that measurement errors and disturbance issues may have been greater for the manual pole dataset than for the cameras. In other words, the manual pole dataset does not represent a perfect test dataset for the cameras, and may if anything contain larger errors. As a result, we cannot yet define measurement uncertainty ranges, although the very high precision, absence of short-term noise and consistent fine-scale responses to water level change (**Figure 10**) all suggest that short-term measurement errors are very low.

However, we do identify two potential issues for the camera method. Firstly, if the combined weight of the camera and the stool on which it is mounted could accelerate rates of compaction. While this would have negligible impacts on measured short-term motion, it could lead to an over-estimate of long-term subsidence. While we sought to minimize this issue by limiting the weight of the system and distributing it across four ground anchors, the deviation of camera-derived vs. manual subsidence values below a 1:1 line in **Figure 7** does provide some suggestion that accelerated compaction could be occurring. On the other hand, the gradient of the relationship is strongly influenced by five data points from the strongly subsiding Misik Oil Palm site, where we found that WTD at the camera site was on average 25 cm deeper than at the manual pole sites, which suggests that higher subsidence rates at the camera site may be real. In almost two years of operation we did not find any visual evidence of accelerated subsidence beneath the cameras compared to the area immediately surrounding each stool. A second issue of concern for the camera method is the

possibility that, at highly rooted forest sites, the ground screws could anchor into the root network rather than the peat matrix. This could for example have contributed to the very limited peat motion observed at the UPR Forest site, where we unfortunately did not have suitable manual pole data to determine whether this apparent stability was real. However, if as seems likely the surface tree roots are moving vertically along with the peat matrix, then this would not lead to an error in the elevation data. These and other potential methodological issues will be addressed through ongoing operation and testing of the cameras in Kalimantan, as well as increased testing in other climate regions, ecosystems and peat types.

Insights Into Peatland Dynamics

As detailed in the introduction, the concept of ‘bog breathing’ is well established in the peatland literature, and forms part of the self-regulatory mechanism of natural peatlands. It has also been identified as a potential measure of peat condition, including evaluating the impacts of land-use and restoration as the seasonal amplitude and dynamics of surface oscillation vary as a function of management (e.g., Howie and Hebda, 2018). Due to the reliance of most studies on less frequent manual measurements, however, rather few studies have been able to assess the short-term dynamics of peat motion. Strack et al. (2006) used a mechanical method to measure surface elevation changes in a Canadian fen, and found that water table fluctuations explained 81–99% of surface level variations on shorter timescales (sub-weekly) whereas the accumulation of entrapped gas bubbles, by increasing peat buoyancy, caused the surface level to rise by up to 8 cm over longer periods, followed by rapid decreases when gases were released. For an undrained peatland in New Zealand, Fritz et al. (2008) recorded a mean annual surface oscillation of 15 cm, again driven largely by variations in water level, but with pronounced seasonal variations in behavior. In the wet season, surface oscillation was large and rapid in response to water level variation, and was attributed to floatation of the peat. In the dry season, elevation changes were smaller, and strongly lagged relative to water level changes, which the authors suggested was because elevation changes at these times were the result of compression and shrinkage. This hysteresis of elevation response to water level changes has been observed elsewhere, and over a range of timescales from individual rain events to seasons (e.g., Howie and Hebda, 2018). Zanello et al. (2011) also observed a strong dependency of short-term peat elevation change on WTD in a drained Italian peatland, with both water table and elevation changing rapidly, and with little evidence of hysteresis, in response to individual rain events.

Compared to these previous studies, ours is the first to provide insights into the high-frequency dynamics of multiple sites with contrasting land-use, as well as being the first from a tropical peatland system. Consistent with previous results, we find that WTD exerts a strong seasonal (**Figure 9**) and episodic (**Figure 10**) influence on peat elevation. These effects operate across a management gradient, from forests to drained agricultural land, although they were least evident in the forest sites. In the short-term, we observed the greatest response to

individual rain events in the deep-drained agricultural and plantation sites, where both water table and peat elevation rapidly rose in response to individual rain events, followed by a rapid decline to pre-event levels. This 'spiky' behavior, with little or no hysteresis between water table and peat elevation, resembles that observed for a drained cropland by Zanello et al. (2011), and reflects the efficient drainage of these systems. Similar but smaller-amplitude variations were observed in the less well-drained Hampangen Oil Palm site, while the burned scrubland sites, which lack active drainage, showed a more damped response, and some evidence of hysteresis. The lack of short-term elevation variation at the UPR Forest site contrasts with the more dynamic behavior observed in undisturbed temperate and boreal peatlands (Strack et al., 2006; Fritz et al., 2008; Howie and Hebda 2018). Tropical peat swamp forests differ from high-latitude peatlands in their dense vegetation cover, dense root layers and high lateral hydraulic conductivity, which could lead to differences in their capacity to move vertically in response to hydrological variations, although longer-term subsidence data do suggest that they respond dynamically to climatic variations on a multi-year timescale (Evans et al., in prep.). At this stage, we cannot rule out a possible methodological artifact as an explanation for the lack of measured short-term surface motion at the forest sites.

On longer timescales, we again observed major differences between sites under different management, and also between years, with the severe 2019 dry season leading to much greater peat shrinkage than the much wetter equivalent period in 2020 at all sites. As on episodic timescales, seasonal variations in peat surface elevation were strongly linked to water table and the overall degree of site drainage, with the deep-drained Misik Agriculture and oil palm sites experiencing elevation decreases of over 6 cm at the peak of the 2019 dry season. The burned sites, which are subject to unregulated drainage, also underwent substantial shrinkage at this time, whereas it appears that the poorly drained Hampangen Oil Palm and irrigated Kalampangan Agriculture sites were less affected (see below). The forest sites appeared (subject to the caveat noted above) to show the least vertical oscillation, consistent with apparently smaller water table drawdown. Since both the amplitude and rate of peat elevation change in response to rainfall events were clearly linked to peat hydrological status and management, our results suggest that monitoring of peat motion could provide an effective and low-cost basis for monitoring peat condition, including the outcome of restoration measures. Since peat elevation changes can also be detected using interferometric synthetic aperture radar (Alshammari et al., 2018; Hoyt et al., 2020) this finding opens up the possibility that satellite measurements of peat motion could, by linking with ground observations, provide a basis for the large-scale assessment of peat condition, and associated metrics including carbon balance.

Over the full period of measurements, we found clear evidence of net subsidence at some sites, and no evidence of accumulation at any site. Whereas Zanello et al. (2011) used a modeling approach to separate the 'reversible' and 'irreversible' elevation change, here we simply compared to the mean elevations during stable periods of the wet seasons at the start

of 2019 and 2020. Nevertheless, it is clear that peat elevation at the deep-drained sites did not rebound in 2020 to the levels observed before the 2019 dry season, suggesting that the severe dry conditions encountered (WTDs of 2 m or more) led to irreversible compaction and peat oxidation. On the other hand, for the wetter 2020 dry season, net subsidence appears to have been minor at most sites, with the exception of the RePeat Burned site (where it remained much smaller than in 2019). Again, it appears subsidence was much lower at the irrigated Kalampangan site, and did not occur at the high water table Hampangen Oil Palm plantation, or at the two forest sites.

Implications for Tropical Peatland Management and Climate Change Mitigation

Given that the method presented here is new, is still undergoing testing and refinement, and that two years represents a relatively short study period, we recognize that caution is needed when interpreting our results. Nevertheless, both short-term (episodic) and longer-term (seasonal and between-year) measurements of peat elevation change obtained by the camera system appear to provide information relevant to the understanding the effects of land-management on peat condition and function. In particular, the evidence of net subsidence at the more deeply drained sites are likely to be at least partly attributable to peat oxidation, rather than temporary shrink/swell, or longer-term compaction; most studies of tropical peatlands have concluded that over 50% of long-term subsidence in drained systems is due to oxidation (Murayama and Bakar, 1996; Hooijer et al., 2012). As high rates of peat oxidation are in turn associated with high CO₂ emissions, our observations from the Misik sites are consistent with other evidence that deep-drained tropical peatlands under plantation agriculture are major GHG emission sources (e.g., Tonks et al., 2017; Cooper et al., 2020; Jauhiainen et al., 2012; Carlson et al., 2017). Moderate to high subsidence levels at the burned sites suggest that these areas, which have unregulated drainage and are subject to dry season water table drawdown and wet season flooding (Figure 9) are also significant CO₂ emission sources. Conversely, low net subsidence at Hampangen and Kalampangan following the severe 2019 dry season suggest that these sites are likely to be much smaller CO₂ sources. At Hampangen this can be attributed to generally high water levels in the peat. While likely to be sub-optimal for productivity, we note that the mean WTD at this site, -0.37 m over the period November 2018 to September 2020, is in line with the Government of Indonesia's '40 cm' regulations for peatland protection (most recently SK.22/PPKL/PKG/PKL, July 0, 2017). At the Kalampangan Agricultural site, this was unlikely to have been the case during the 2019 dry season, when ditch water levels were observed to be below 2 m, yet subsidence (and by inference CO₂ emissions) seem to have been at least partly mitigated by surface irrigation. Although undertaken to support crop production, it is possible that this maintained moisture levels in the upper peat layer at a sufficient level to restrict oxidation. If correct, this has significant implications, as the Indonesian Peat Restoration Agency (BRG) has installed over 10,000 wells in

community-owned peatland areas since 2016 (BRG, 2019). These wells were constructed primarily to provide a source of water for fighting peat fires. However, in areas where water can be sustainably extracted from mineral aquifers below the peat, and used to maintain peat surface moisture levels during dry periods, it is possible that this could generate substantial emissions mitigation (as well as supporting crop production). To our knowledge, surface irrigation has not been considered previously as a form of climate change mitigation in tropical peatlands. While there are clearly risks in extracting water from aquifers below the peat, as well as financial and energy costs, the potential for targeted irrigation to reduce peat subsidence and carbon loss appears to merit further attention.

More generally, for peat under both oil palm and other agricultural cultivation, it is clear from our results that differences in water management between sites led to different rates of subsidence, and therefore likely to different rates of CO₂ emissions. While subsidence rates are less directly connected to methane (CH₄) emissions, these tend to be highest at permanently or seasonally waterlogged sites, where wetland-adapted plant species are present, and negligible when WTD exceeds 20–30 cm (Couwenberg et al., 2011). Information on WTD and peat elevation change obtained from the peat cameras, together with vegetation characteristics may therefore also be of use for inferring rates of CH₄ emission. At present, Intergovernmental Panel on Climate Change Tier 1 emissions inventory reporting methods (IPCC, 2014) provide only a single set of ‘emission factors’ for tropical peatlands under oil palm plantation, and another set of emission factors for tropical peatlands under all cropland other than paddy rice. In accordance with assessments of CO₂ and CH₄ fluxes from high-latitude peatlands (Couwenberg et al., 2011; Tiemeyer et al., 2020), as well as analyses of long-term subsidence from tropical peatlands (Hooijer et al., 2012; Evans et al., 2019) our analysis suggests that both subsidence and GHG emissions vary greatly within each land-use category, depending on the water management. This is important, as it suggests that measures aimed at raising water levels or increasing near-surface soil moisture levels could—while unlikely to halt emissions entirely—generate substantial climate change mitigation benefits via reduced CO₂ emissions, which cannot currently be captured via IPCC Tier 1 inventory reporting methods. The development of more sophisticated ‘Tier 2’ reporting methods, describe the effects of improved water management in managed tropical peatland landscapes, would enable the benefits of these mitigation measures to be captured in project level and national level emissions reporting, and might therefore help to reconcile the competing objectives of climate change mitigation and enhancement of livelihoods in these threatened, carbon-rich ecosystems.

CONCLUSION

The ‘peat camera’ system described in this paper has provided new insights into the behavior of tropical peatlands, revealing a range of highly dynamic peat behaviors on timescales ranging

from sub-daily to annual, and linked to management, hydrological and climatic factors. It offers an accurate, reliable and low-maintenance method for simultaneous measurement of peat elevation and water table change, and may also be an effective proxy measure of the peatland carbon balance. The simplicity and low cost of the system (in the region of USD 300) compares favourably to commercial systems for monitoring peat motion and water table, and is orders of magnitude cheaper than eddy covariance systems for CO₂ flux monitoring. At present, the method has only been tested at a small number of sites, and over a limited time period, during which we made a number of modifications to improve reliability and reduce data loss, but the system requires further testing and refinement, and streamlining of the image data processing. Provided that these challenges can be overcome, we believe that the method has widespread potential application, particularly for monitoring of peatlands in remote areas, by groups with limited budgets for research and monitoring, and at a greater number of locations than could be achieved at the same cost using existing technologies. Increasing the spatial coverage of observations could in turn facilitate the implementation of satellite-based monitoring systems by providing robust and representative ground-based calibration and test data. Such large-scale and effective monitoring is urgently required to support the future management, mitigation of GHG emissions and restoration of one of the terrestrial biosphere’s most distinctive ecosystems, and largest carbon stores.

DATA AVAILABILITY STATEMENT

The raw data supporting the conclusions of this article will be made available by the authors, without undue reservation.

AUTHOR CONTRIBUTIONS

CE led the study and drafted the manuscript with AJ-S. The peat motion camera concept was conceived by AG in discussion with CE, and the system was designed and tested by NC, with additional refinements by AJ-S and AJ. Image processing scripts were written by ZM with support from AG. AJ and AJ-S led the Central Kalimantan field deployments, and AJ led manual subsidence measurements. LK, ML, KK, and MH contributed to wider system deployment and testing. SS, SP, and SE contributed to the establishment of the field program via the PASSES and SUSTAINPEAT projects, and provided expertise on peatland processes. AJ-S, JW, and AR undertook image processing, quality assurance and data management. All authors read, commented on and contributed to the final manuscript.

FUNDING

The development and operation of the peat motion cameras was undertaken as part of the project PASSES: Peatland Assessment

in Southeast Asia by Satellite, funded by the United Kingdom Space Agency International Partnership Program. Field deployments in Central Kalimantan were undertaken at field sites established by the project SUSTAINPEAT: Overcoming barriers to sustainable livelihoods and environments in smallholder agricultural systems on tropical peatland, funded by United Kingdom Research and Innovation via the Global Challenges Research Fund and the Biotechnology and Biological Sciences Research Council (BBSRC) Grant number BB/P023533/1. CE received additional support from the UK Natural Environment Research Council grant Sustainable Use of Natural Resources to Improve Human Health and Support Economic Development (SUNRISE, Grant No. NE/R000131/1) ML was supported by a Natural Environment Research Council PhD studentship as part of the STARS Doctoral Training Center (Grant number NE/M009106/1). Groundwater level data used at

the RePeat Burned site (December 2018 to September 2019) were obtained from the SATREPS: Science and Technology Research Partnership for Sustainable Development project 'Wild fire and carbon management in peat-forest in Indonesia' funded by Japan Science and Technology Agency and Japan International Cooperation Agency.

ACKNOWLEDGMENTS

We are grateful to the Ministry of Research Technology and Higher Education of Indonesia (RISTEKDIKTI) for their support of the SUSTAINPEAT project. We would also like to thank the University of Palangka Raya field staff who supported the measurement program, and the landowners who hosted our field equipment.

REFERENCES

- Alshammari, L., Large, D. J., Boyd, D. S., Sowter, A., Anderson, R., Andersen, R., et al. (2018). Long-term peatland condition assessment via surface motion monitoring using the ISBAS DInSAR technique over the Flow Country, Scotland. *Remote Sensing*, 10, 1103. doi:10.3390/rs10071103
- BRG (2019). Three years of peat restoration indonesia badan restorasi gambut. Available at: https://brg.go.id/wp-content/uploads/2019/06/3-years-peatland-restoration-inindonesia_eng-pmk_without-track-changes_edit-layout.pdf. (Accessed November 15, 2020)
- Carlson, K. M., Gerber, J. S., Mueller, N. D., Herrero, M., MacDonald, G. K., Brauman, K. A., et al. (2017). Greenhouse gas emissions intensity of global croplands. *Nat. Clim. Change* 7, 63–68. doi:10.1038/NCLIMATE3158
- Cheyne, S. M., Sastramidjaja, W. J., Muhahir Rayadin, Y., and MacDonald, D. W. (2016). Mammalian communities as indicators of disturbance across Indonesian Borneo. *Glob. Ecol. Conserv.* 7, 157–173. doi:10.1016/j.gecco.2016.06.002
- Cooper, H. V., Evers, S., Aplin, P., Crout, N., Bin Dalahan, M. P., and Sjögersten, S. (2020). Greenhouse gas emissions resulting from conversion of peat swamp forest to oil palm plantation. *Nat. Commun.* 11, 407. doi:10.1038/s41467-020-14298-w
- Couwenberg, J., Thiele, A., Tanneberger, F., Augustin, J., Bärtsch, S., Dubovik, D., et al. (2011). Assessing greenhouse gas emissions from peatlands using vegetation as a proxy. *Hydrobiologia* 674, 67–89. doi:10.1007/s10750-011-0729-x
- Dargie, G. C., Lewis, S. L., Lawson, I. T., Mitchard, E. T., Page, S. E., Bocko, Y. E., et al. (2017). Age, extent and carbon storage of the central Congo Basin peatland complex. *Nature* 542, 86–90. doi:10.1038/nature21048
- de Louw, P. G., Bootsma, H., Kooi, H., Kramer, M., and Erkens, G. (2018). Land subsidence by peat oxidation leads to enhanced salinization through boils in Dutch polders. *E3S Web Conf.* 54, 00007. doi:10.1051/e3sconf/20185400007
- Deverel, S. J., and Leighton, D. A. (2010). Historic, recent, and future subsidence, sacramento-san Joaquin delta, California, USA. *San Francisco Estuary Watershed Sci.* 8, 1–23. doi:10.15447/sfews.2010v8iss2art1
- Dise, N. B. (2009). Environmental science peatland response to global change. *Science* 326, 810–811. doi:10.1126/science.1174268
- Dommain, R., Couwenberg, J., Glaser, P. H., Joosten, H., and Suryadiputra, I. N. N. (2014). Carbon storage and release in Indonesian peatlands since the last deglaciation. *Quat. Sci. Rev.* 97, 1–32. doi:10.1016/j.quascirev.2014.05.002
- Erkens, G., van der Meulen, M. J., and Middelkoop, H. (2016). Double trouble: subsidence and CO₂ respiration due to 1,000 years of Dutch coastal peatlands cultivation. *Hydrogeology J.* 24, 551–568. doi:10.1007/s10040-016-1380-4
- Evans, C. D., Page, S. E., Jones, T., Moore, S., Gauci, V., Laiho, R., et al. (2014). Contrasting vulnerability of drained tropical and high-latitude peatlands to fluvial loss of stored carbon. *Glob. Biogeochem. Cycles* 28, 1215–1234. doi:10.1002/2013gb004782
- Evans, C. D., Williamson, J. M., Kacaribu, F., Irawan, D., Suardiwerianto, Y., Hidayat, M. F., et al. (2019). Rates and spatial variability of peat subsidence in Acacia plantation and forest landscapes in Sumatra, Indonesia. *Geoderma* 338, 410–421. doi:10.1016/j.geoderma.2018.12.028
- FAOSTAT (2018). *Food and agriculture organisation of the united nations*. Rome: FAOSTAT.
- Fiaschi, S., Holohan, E. P., Sheehy, M., and Floris, M. (2019). PS-InSAR analysis of Sentinel-1 data for detecting ground motion in temperate oceanic climate zones: a case study in the Republic of Ireland. *Remote Sens.* 11, 348. doi:10.3390/rs11030348
- Friedlingstein, P., Jones, M., O'sullivan, M., Andrew, R., Hauck, J., Peters, G., et al. (2019). Global carbon budget 2019. *Earth Syst. Sci. Data* 11, 1783–1838. doi:10.5194/essd-11-1783-2019
- Fritz, C., Campbell, D. L., and Schipper, L. A. (2008). Oscillating peat surface levels in a restiad peatland, New Zealand—magnitude and spatiotemporal variability. *Hydrol. Process.* 22, 3264–3274. doi:10.1002/hyp.6912
- Hirano, T., Segah, H., Kusin, K., Limin, S., Takahashi, H., and Osaki, M. (2012). Effects of disturbances on the carbon balance of tropical peat swamp forests. *Glob. Change Biol.* 18, 3410–3422. doi:10.1111/j.1365-2486.2012.02793.x
- Hooijer, A., Page, S., Jauhiainen, J., Lee, W. A., Lu, X. X., Idris, A., et al. (2012). Subsidence and carbon loss in drained tropical peatlands. *Biogeosciences* 9, 1053–1071. doi:10.5194/bg-9-1053-2012
- Howie, S. A., and Hebda, R. J. (2018). Bog surface oscillation (mire breathing): a useful measure in raised bog restoration. *Hydrol. Process.* 32, 1518–1530. doi:10.1002/hyp.11622
- Hoyt, A. M., Chaussard, E., Seppäläinen, S. S., and Harvey, C. F. (2020). Widespread subsidence and carbon emissions across Southeast Asian peatlands. *Nat. Geosci.* 13, 435–440. doi:10.1038/s41561-020-0575-4
- Hutchinson, J. N. (1980). Record of peat wastage in the east-anglian fenlands at Holme Post, 1848–1978 AD. *J. Ecol.* 68, 229–249.
- IPCC (2014). *2013 supplement to the 2006 IPCC guidelines for national greenhouse gas inventories: Wetlands*. Switzerland: Intergovernmental Panel on Climate Change.
- Jauhiainen, J., Hooijer, A., and Page, S. E. (2012). Carbon dioxide emissions from an *Acacia* plantation on peatland in Sumatra, Indonesia. *Biogeosciences* 9, 617–630. doi:10.5194/bg-9-617-2012
- Leifeld, J., and Menichetti, L. (2018). The underappreciated potential of peatlands in global climate change mitigation strategies. *Nat. Commun.* 9, 1071. doi:10.1038/s41467-018-03406-6
- Marshall, C., Large, D. J., Athab, A., Evers, S. L., Sowter, A., Marsh, S., et al. (2018). Monitoring tropical peat related settlement using ISBAS InSAR, Kuala Lumpur International Airport (KLIA). *Eng. Geology*. 244, 57–65. doi:10.1016/j.enggeo.2018.07.015
- Morton, P. A., and Heinemeyer, A. (2019). Bog breathing: the extent of peat shrinkage and expansion on blanket bogs in relation to water table, heather management and dominant vegetation and its implications for carbon stock assessments. *Wetlands Ecol. Manage.* 27, 467–482. doi:10.1007/s11273-019-09672-5

- Murayama, S., and Bakar, Z. A. (1996). Decomposition of tropical peat soils, estimation of *in situ* decomposition by measurement of CO₂ flux. *Jarq-jpn. Agr. Res. Q.* 30, 153–158.
- Page, S. E., Siegert, F., Rieley, J. O., Boehm, H. D., Jaya, A., and Limin, S. (2002). The amount of carbon released from peat and forest fires in Indonesia during 1997. *Nature* 420, 61–65. doi:10.1038/nature01131
- Page, S. E., and Baird, A. J. (2016). Peatlands and global change: response and resilience. *Annu. Rev. Environ. Resour.* 41, 35–57. doi:10.1146/annurev-environ-110615-085520
- Page, S. E., Rieley, J. O., and Banks, C. J. (2011). Global and regional importance of the tropical peatland carbon pool. *Glob. Change Biol.* 17, 798–818. doi:10.1111/j.1365-2486.2010.02279.x
- Page, S., Hoscilo, A., Wösten, H., Jauhainen, J., Silvius, M., Rieley, J., Ritzema, H., et al. (2009). Restoration ecology of lowland tropical peatlands in Southeast Asia: current knowledge and future research directions. *Ecosystems* 12, 888–905. doi:10.1007/s10021-008-9216-2
- Rublee, E., Rabaud, V., Konolige, K., and Bradski, G. (2011). ORB: an efficient alternative to SIFT or SURF. in Proceedings of the IEEE international conference on computer vision (ICCV). Barcelona, Spain.
- Smith, P. (2014). “Agriculture, forestry and other land use (AFOLU),” in *Climate change 2014: mitigation of climate change. Contribution of working group III to the fifth assessment report of the intergovernmental panel on climate change.* (Cambridge, United Kingdom and New York, NY: Cambridge University Press).
- Stephens, J., Allan, L., and Chen, E. (1984). Organic soil subsidence. *Rev. Eng. Geology.* 6, 107–122.
- Strack, M., Kellner, E., and Waddington, J. M. (2006). Effect of entrapped gas on peatland surface level fluctuations. *Hydrol. Process.* 20, 3611–3622. doi:10.1002/hyp.6518
- Strack, M., and Waddington, J. M. (2007). Response of peatland carbon dioxide and methane fluxes to a water table drawdown experiment. *Glob. Biogeochem. Cycles* 21, GB1007. doi:10.1029/2006gb002715
- Susanti, R. D., and Anjasmara, I. M. (2019). Analysing peatland subsidence in Pelalawan Regency, Riau using DInSAR method. *IPTEK J. Proc. Ser.* 2, 60–64. doi:10.12962/j23546026.y2019i2.5308
- Tiemeyer, B., Freibauer, A., Borraz, E. A., Augustin, J., Bechtold, M., Beetz, S., et al. (2020). A new methodology for organic soils in national greenhouse gas inventories: data synthesis, derivation and application. *Ecol. Indicators* 109, 105838. doi:10.1016/j.ecolind.2019.105838
- Tonks, A. J., Aplin, P., Beriro, D. J., Cooper, H., Evers, S., Vane, C. H., et al. (2017). Impacts of conversion of tropical peat swamp forest to oil palm plantation on peat organic chemistry, physical properties and carbon stocks. *Geoderma.* 289, 36–45. doi:10.1016/j.geoderma.2016.11.018
- Turetsky, M. R., Benscoter, B., Page, S., Rein, G., van der Werf, G. R., and Watts, A. (2015). Global vulnerability of peatlands to fire and carbon loss. *Nat. Geosci.* 8, 11–14. doi:10.1038/ngeo2325
- Wösten, J. H. M., Ismail, A. B., and Van Wijk, A. L. M. (1997). Peat subsidence and its practical implications: a case study in Malaysia. *Geoderma.* 78, 25–36.
- Wijedasa, L. S., Sloan, S., Page, S. E., Clements, G. R., Lupascu, M., and Evans, T. A. (2018). Carbon emissions from South-East Asian peatlands will increase despite emission-reduction schemes. *Glob. Chang Biol.* 24, 4598–4613. doi:10.1111/gcb.14340
- Zanello, F., Teatini, P., Putti, M., and Gambolati, G. (2011). Long term peatland subsidence: experimental study and modeling scenarios in the Venice coastland. *J. Geophys. Res.* 116, F04002. doi:10.1029/2011JF002010
- Zhou, Z., Li, Z., Waldron, S., and Tanaka, A. (2019). InSAR time series analysis of L-band data for understanding tropical peatland degradation and restoration. *Remote Sens.* 11, 2592. doi:10.3390/rs11212592

Conflict of Interest: The authors declare that the research was conducted in the absence of any commercial or financial relationships that could be construed as a potential conflict of interest.

Copyright © 2021 Evans, Callaghan, Jaya, Grinham, Sjøgersten, Page, Harrison, Kusin, Kho, Ledger, Evers, Mitchell, Williamson, Radbourn and Jovani-Sancho. This is an open-access article distributed under the terms of the Creative Commons Attribution License (CC BY). The use, distribution or reproduction in other forums is permitted, provided the original author(s) and the copyright owner(s) are credited and that the original publication in this journal is cited, in accordance with accepted academic practice. No use, distribution or reproduction is permitted which does not comply with these terms.